EXPERIMENTAL STUDY OF ADMISSION AND EXHAUST FLOW IN A SINGLE-CYLINDER MOTORED ENGINE

Och, Stephan Hennings, stephan.och@pop.com.br
Pontifícia Universidade Católica do Paraná – PUCPR

Velásquez, José Antonio, jose.velasquez@pucpr.br
Pontifícia Universidade Católica do Paraná – PUCPR
Universidade Tecnológica Federal do Paraná – UTFPR

Abstract. This paper contains the description of a physical model, which was built in order to study the non-stationary and non-isentropic flow that occurs in the admission and exhaust ducts of an internal combustion engine. A detailed presentation of the experimental apparatus used is given, including information on the sensors utilized to measure the pressure, the angular position of the crankshaft and the displacement of the valves. The experiments carried out using this physical model adequately reproduced the relevant phenomena observed in real engines. The results of these experiments have been presented and discussed in this paper.

Keywords: Transitory flow of a compressible fluid; Admission and exhaust processes of a combustion engine; Physical model for the study of wave propagation in ducts.

1. INTRODUCTION

The increase in the price of fuels derived from petroleum and the introduction of increasingly restrictive environmental norms has motivated research to develop engines, which are more efficient and less harmful to the environment. If up to the seventies the development of engines was focused on obtaining greater performance, the first oil crisis (1973) and the first signs of fragility of the environment, focused attention on energy efficiency and the reduction of the concentration of pollutants in the exhaust gases.

With the purpose of developing more efficient and less pollutant engines, research is carried out using experimental, theoretical/empirical or computational approaches. Research based on a purely experimental approach is expensive and can be very time consuming until finally producing satisfactory solutions. On the other hand, the theoretical/empirical approach is usually based on the experience accumulated in similar projects, and therefore is of great value at the beginning of the development, however, it is ineffective in producing important technological innovations. Nowadays, the computational approach is without a doubt the most widely used, both in the initial defining phases of the project as well as in its advanced phases. However, this approach demands the use of experimental resources for the confirmation of the results predicted by computational models.

The study of internal combustion engines requires that the computational models adequately represent the engine processes. Therefore, the computational model must be verified using experimental data that can be obtained from a simplified physical model or from an engine functioning in its full complexity. When using a simplified physical model, it is necessary that the phenomena under analysis should be adequately reproduced in it. This is the basic reason that motivated the present work: the construction of a physical model that allows both the study of a non-stationary and non-isentropic flow, which is typical of the admission and exhaust processes of an engine, as well as the measurement with adequate precision of the most relevant parameters of this flow.

2. EXPERIMENTAL APPARATUS

2.1. The test bench

The physical model was built from a spark ignition, single-cylinder, four-stroke engine, with the carburetor, the muffler and the exhaust duct removed. Instead of these elements, cylindrical admission and exhaust ducts were placed, each one being 1 meter long and 25.4 mm in diameter, which were attached as extensions of the admission and exhaust ports. With the purpose of studying the phenomenon, pressure waves were induced in these ducts by motoring the combustion engine with the help of an electric engine, whose rotation speed was controlled by a frequency inverter. Figure 1 shows the main components of the test bench.

2.2 Measurement of the valve displacement

The opening and closing moments of the valves as well as their displacement curves are important parameters for the study of the flow in the admission and exhaust ducts of an internal combustion engine. These moments, which can be determined from the displacement curve and are generally expressed in terms of the angular position of the crankshaft, determine how long the ducts are subject to the influence of the conditions found in the cylinder.

Figure 1 – The physical model.

To obtain the displacement curve of the valves it was necessary to use a measurement system with the following characteristics: *(i)* capability of measuring displacements of up to 7 mm; *(ii)* immunity to impact; *(iii)* capability of making high frequency measurements; and *(iv)* capability of correlating the valve displacement to the crankshaft angular position. Considering the facilities available in the Laboratory of Applied Thermodynamics at PUCPR, the system that was better adjusted to such requirements was a laser interferometer operating together with the optic angular marker AVL 364, both connected to a computer equipped with an analog-digital converter (Indimeter 617). The main advantage of this system is that there is no mechanical contact with the valve, since if the measurement were not done this way the measuring instrument could be damaged, due to the high acceleration to which the valves are subject. Moreover, the composition of the measuring system was facilitated because the response characteristic of the laser interferometer was within the range ±10 V, proving itself compatible to the digital-analog converter utilized. Taking into consideration that the interval of data digitalization is controlled by the optic angular marker, which produces a pulse every 0.5° of crankshaft rotation, the time interval between two consecutive measurement registers results

$$\Delta t = \frac{0,5}{6\,rpm} \tag{1}$$

Thus, when the engine is running at 600 rpm and at 3600 rpm (the minimum and maximum engine speeds in the experiments) the time interval between two consecutive measurements results $1,34\times10^{-4}$ s and $2,3\times10^{-5}$ s, respectively. It is evident, therefore, that the measuring demands high rates of data acquisition.

Figure 2 shows the elements of the system used for measuring the valves displacement. The laser beam strikes a reflective element placed over the valve in movement and due to the Doppler effect, it modifies its frequency. This frequency variation is identified by the photo detectors and converted by the counter into a voltage signal, which can be used to measure both the valve displacement and the valve speed. In the experiments that were carried out in this project, the direct measurement of the displacement revealed itself inadequate, for it was observed that the greatest displacement of the valve (7 mm) coincides with the measurement limit of the interferometer, leading to its saturation and consequent loss of the reference of the output signal. To overcome this problem, the solution found was to work with the signal proportional to the valve speed and integrate this signal in order to produce the displacement.

The measurement of the valve displacement was registered in relation to the angular position of the crankshaft with the use of an optic angular marker. The principle of the functioning of this equipment is based on the photoelectric tracing of a radial sequence of traces and gaps, carried out on a glass disk, having constituted what is named an incremental track. When a light beam strikes the incremental track, the radial sequence of traces and gaps produces light pulses whose duration depends on the angular displacement between the traces. The photovoltaic cells of the light-pulse converter receive this light signal and transform it into an electric signal. A second incremental track on the glass disk is used to produce a single pulse that serves as a reference to define the angular position adopted as zero. The signals emitted by the angular marker are conducted to the analog-digital converter, which uses the angular displacement signal to control the time interval between two consecutive measurements of the valve speed and the reference signal to restart the counting of the angular position when a cycle is completed.
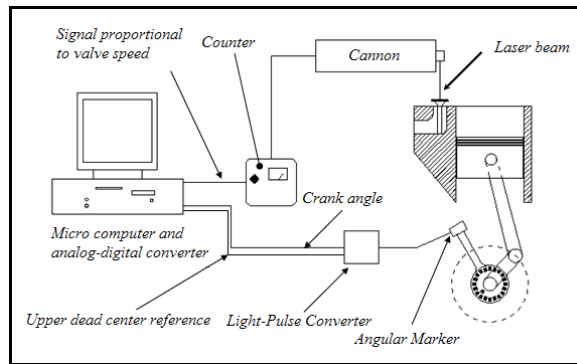
Figure 2 – Measuring system of valve speed.

2.3 Pressure measuring

The measurement of the pressure in the combustion chamber as well as in the admission or exhaust ducts of internal combustion engines requires transducers that allow high frequency measurements and present linearity in a wide pressure range, even when submitted to high temperatures (Bueno, 2006). Measuring pressure using piezoelectric crystals may be more costly, but the results are more precise than the results obtained when using a strain gauge as measuring device, especially when the sensors are subject to high temperatures. For this reason the piezoelectric transducers are widely used in determining engine indicator diagrams, whereas the strain gauges (metallic or piezo-resistive) are used in situations where the temperature is moderate, for example in the measurement of the pressure in the fuel injection line. However, literature also reports drawbacks inherent to the use of piezoelectric pressure sensors, such as instability of the base line and low intensity in the output signal.

Figure 3 shows the basics of the functioning of a piezoelectric pressure sensor. The variation of the pressure applied to the diaphragm results in a variation of the force acting on the piezoelectric crystal, promoting an alteration in its state of deformation and, by the piezoelectric effect, the polarization of charges at a rate i, which is the output signal of the transducer.

$$i = \frac{dq}{dt} = -G_s \frac{dP}{dt} \tag{2}$$

where G_s is the transducer sensitivity.

In the experiments carried out in this project, the in-cylinder pressure as well as the pressure at various points along the exhaust and admission ducts, were measured. In order to measure the in-cylinder pressure an AVL 12QP300CV piezoelectric pressure transducer was installed in the combustion chamber through the spark-plug orifice. In addition, the pressure along the ducts was measured using an AVL GM12D piezoelectric transducer, installed with the aid of adapters welded on to the ducts. Table 1 shows the characteristics of the pressure transducers, whereas Figure 4 shows the installation points of the pressure sensor along the ducts.
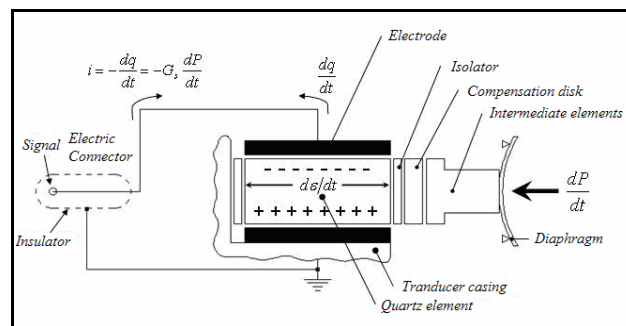

Figure 3 – The piezoelectric pressure transducer

Table 1 – Piezoelectric pressure transducers data

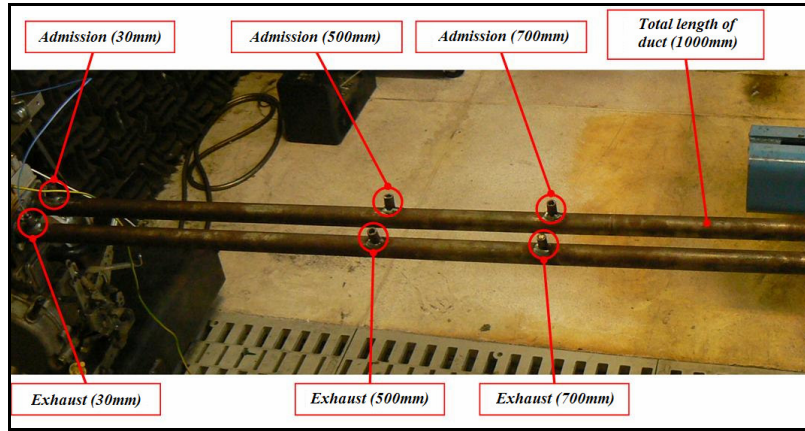|	AVL 12QP300CV	AVL GM12D
Base scale (*bar*)	120	200
Sensitivity (*pC/bar*)	44,30	16,41
Linearity	< ±0,5%	< ±0,3%
Natural Frequency (*kHz*)	110	130

Figure 4 – Location of the measuring points along the duct.

2.4 The data acquisition system

Figure 5 presents a simplified diagram of the path followed by the signal emitted by the piezoelectric sensor. A shielded cable of high insulation resistance carries the charges polarized by the transducer towards the negative input of the charge amplifier, also named as piezoelectric amplifier. This cable must be of low electric resistance so that loss of signal strength does not occur and, in addition, has to be shielded in order to avoid signal distortion due to electromagnetic interference. The charge amplifier should exhibit high input impedance, thus preventing the passing of the electric current through it, and at the same time, forcing the current to flow through the capacitor connected between the negative input and the exit of the amplifier. Thus, the tension U in the circuit is related to the current i as follows

$$\frac{dU}{dt} = \frac{1}{G_a} \cdot i \tag{3}$$

where G_a is the capacitance of the capacitor. Integrating Equation 3, results

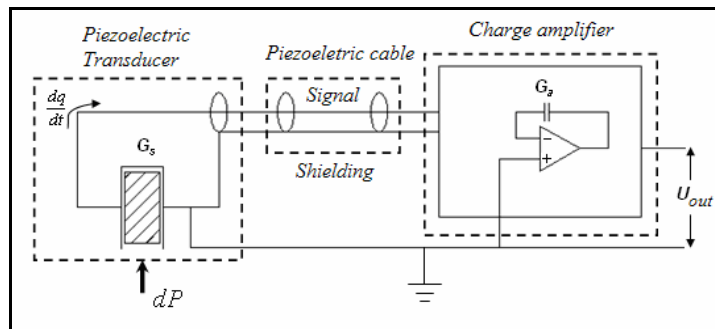$$U - U_{ref} = \frac{1}{G_a} \int i \, dt \tag{4}$$

Figure 5 - Conditioning of the signal emitted by the pressure transducer.

where U_{ref} is the reference tension, which is assumed to be nil because the amplifier is grounded. Equation (4) shows that the amplifier output voltage is inversely proportional to the capacitor capacitance G_a (amplifier gain) and directly proportional to the time integral of the current (this is the reason the term 'integrating circuit' is used for this configuration). Combining Equations (2) and (4) results

$$U = \frac{G_s}{G_a}\left(P - P_{ref}\right)$$ (5)

Deriving Equation (5) in relation to the pressure and taking into account that the sensitivity S of a measurement system is defined as the variation of the response characteristic divided by the variation of the input characteristic, the following expression can be obtained

$$S = \frac{dU}{dP} = \frac{G_s}{G_a}$$ (6)

Thus, the sensitivity of the pressure measuring system is given by the ratio of the sensor gain to the amplifier gain. If these gains are constant, the sensitivity will also be a constant and the output characteristic will vary linearly in relation to the input characteristic. Moreover, considering the convenience of having a high sensitivity measuring system available, it can be verified in Equation (6) that to increase the sensitivity of the system it would be necessary to increase the gain of the sensor and reduce the gain of the amplifier. However, the analog-digital converter is limited to analog signals that vary in a defined range (generally ±10 V), and so as not to exceed the limits the gain value of the amplifier should be chosen appropriately.

It is worth mentioning that the charge polarized by the piezoelectric pressure transducer is very weak, reaching only a few dozens of pC/bar. Therefore, current leakage in the measuring system has a strong impact on the measurement results, causing a slow and continuous decrease of the output voltage. This effect results in underestimated values for pressure, being mentioned in the literature as the pressure data baseline drift or shift (Lancaster, 1975; Lapuerta, 2000; Payri, 2006). This phenomenon causes displacements of the pressure baseline that may reach several bars, requiring the periodic reset of the amplifier to avoid its saturation. In order to reduce this problem to tolerable levels it is necessary to use a high impedance charge amplifier with low current leakage, as well as keeping the electrical connections of the measuring system spotlessly clean. During the experiments the cleaning and resetting of the integrating circuit were made before each of the measurements, as recommended by Bueno (2006).

3. RESULTS

To determine the instantaneous position of the valves, the measurements with the laser interferometer had initially been carried out using the characteristic of response proportional to the displacement. However this method showed itself to be inadequate, for the limit of the interferometer measurements coincided with the maximum displacement of the valves (7 mm), causing a counter saturation and consequently a reference loss of the output signal. The option was to use the characteristic of response proportional to the valve speed, which allowed for a signal of good quality. Each measurement was taken and the data was stored for the maximum number of cycles that the converter can hold (42 cycles) and then the average curve between these cycles was calculated. The result is shown in Figure 6, where the speed curves of the exhaust and admission valves can be seen. Even though these curves were not registered simultaneously, it was easy to combine them in the same graph, for they had the same crank angle reference, the 0 value corresponding to the compression top dead center. The position of this dead center was determined from the in-cylinder pressure curve, using a loss angle equal to 0.7º c.a., as recommended by the manufacturer of the pressure measuring system (AVL, 1997).

The results of the valve speed measurements allowed for the calculation of the displacement by means of a simple numerical integration as follows,

$$x_{i+1} = x_i + \frac{v_i \cdot \Delta\theta}{6 \cdot \omega}$$ (7)

where v is the valve speed, in m/s; ω is the rotation speed of the crankshaft, in rpm; and $\Delta\theta$ is the angular displacement of the crankshaft between two consecutive registers (0,5º). The valve displacement curves obtained after the numerical integration are shown in Figure 6, whereas the angular positions of the crankshaft, corresponding to the opening and closing moments of the valves, are reported in Table 3.
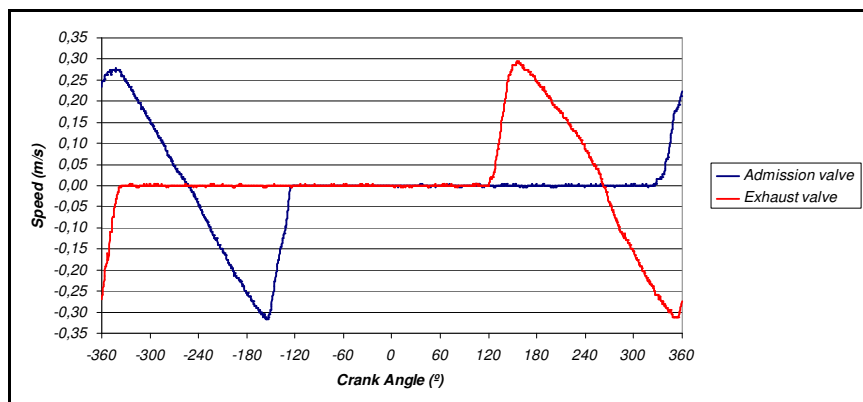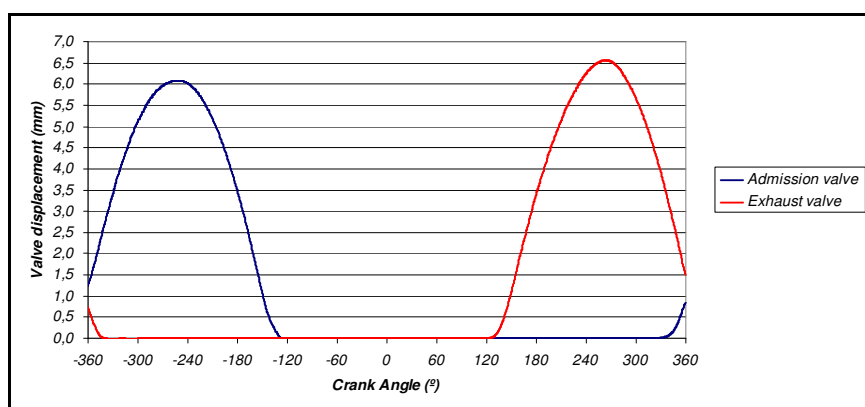
Figure 6 – Admission and exhaust valves speed.

Figure 7 – Admission and exhaust valves displacement.

Table 3 – Valves opening and closing crank angles.

Opening of the admission valve	330,5º
Closing of the admission valve	-123,5º
Opening of the exhaust valve	120,0º
Closing of the exhaust valve	-340,5º

As mentioned above, the measuring of the pressure in the combustion chamber of the engine was carried out with the use of a piezoelectric transducer AVL 12QP300CV. Taking into account the pressure magnitude in the combustion chamber and the saturation limits of the amplifier, a gain of 100 pC/bar was chosen for the charge amplifier. Again in this measurement, data was stored to the maximum number of cycles that the system can storage (42 cycles) and then, the average between these cycles was determined. The results related to four different engine speeds (1400, 1800, 2400 and 2600 rpm) are shown in Figure 8. It is noticeable that the maximum pressure of the averaged cycle increases with the increase of the engine speed, due to the increase of the air mass that enters the cylinder. It should be pointed out that these are pressure curves without combustion, which confers a certain symmetry to the curve during the time when the valves are closed (if the process had been isentropic, this curve would certainly be symmetrical in relation to the pressure axis).

The curves shown in Figure 9 were obtained by altering the pressure range in such a way that the in-cylinder pressure during the admission and exhaust processes is focused. These curves are important for the study of the flow in the ducts, because they show the in-cylinder pressure that affects the waves propagation along the ducts. During the admission process (corresponding to the crankshaft positions between -330,5° and 123,5°), it can be noticed that due to the cylinder filling work, the cylinder pressure falls below the base value (set at zero value). Normally, in engines running with combustion, the in-cylinder pressure at the beginning of the exhaust is still greater than the external pressure, facilitating the blow down. However, in this experiment, as the engine was running motored, the in-cylinder pressure was below the external pressure right at the beginning of the exhaust valve opening, therefore producing an expansion wave in the exhaust duct.
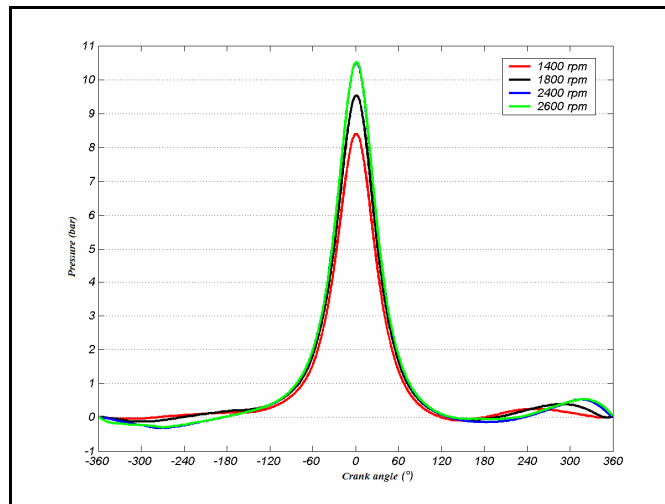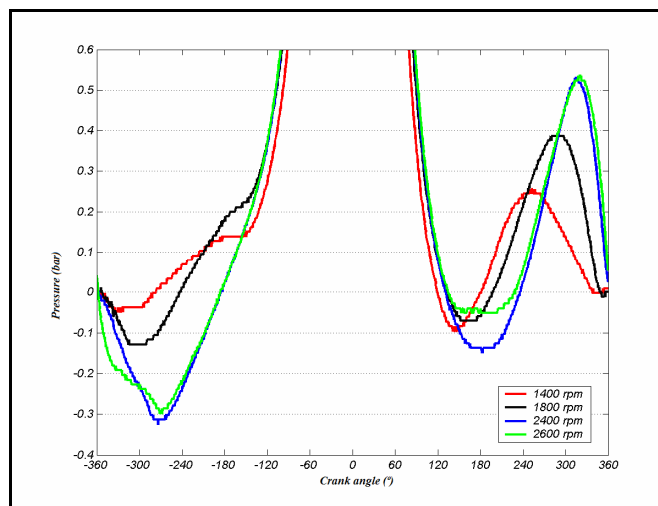
Figure 8 – Pressure in the engine cylinder.

Figure 9 – In-cylinder pressure during the gas exchange process.

The measurements for the pressure in the cylinder and in the ducts were carried out at the same time, since it was possible to use two pressure transducers. The pressure transducer used in the ducts was an AVL GM12D, for which a conversion factor of 3,047 bar/V was obtained when using a gain of 50 pC/V for the charge amplifier. It should be emphasized that the discussion on the pressure variations should be restricted to the measurements in the same sensor position. This is due to the lack of a common reference for the measurements at different sensor positions, since the integration of the pressure signal by the circuit requires a pressure value at one point to be known in order to serve as an integration constant. In the experiments, due to the lack of a pressure reference data, the value of zero was adopted for the pressure at -360º c.a. As this value was arbitrary, the relative comparison between distinct positions should not be made. The solution adopted to resolve this problem consists of using numerical models to adjust the experimental values. This will be done in future projects, as the object of this project is only to supply valid experimental data for future comparisons.

Figure 10 shows the pressure in the cylinder as well as in the measuring positions of the admission duct for a rotation speed of 2600 rpm. The crank angle axis was referred to the valve opening and the cylinder pressure curve is shown up to the valve closing angle. It is possible to observe that from the admission valve opening until crank angle reaches 120º the in-cylinder pressure falls, forcing the entrance of mass to the cylinder, and also that the pressure in the duct accompanies this fall. Beyond this angle, the in-cylinder pressure rises forming a compression wave, which is propagated along the duct diminishing its amplitude due to friction against the duct wall and heat exchange.
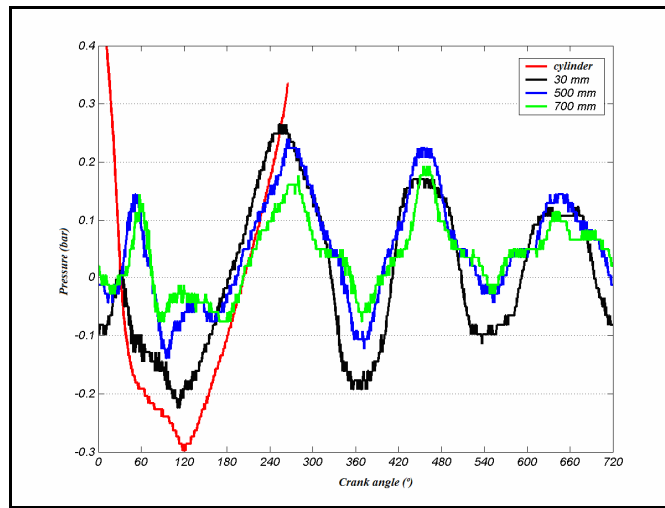
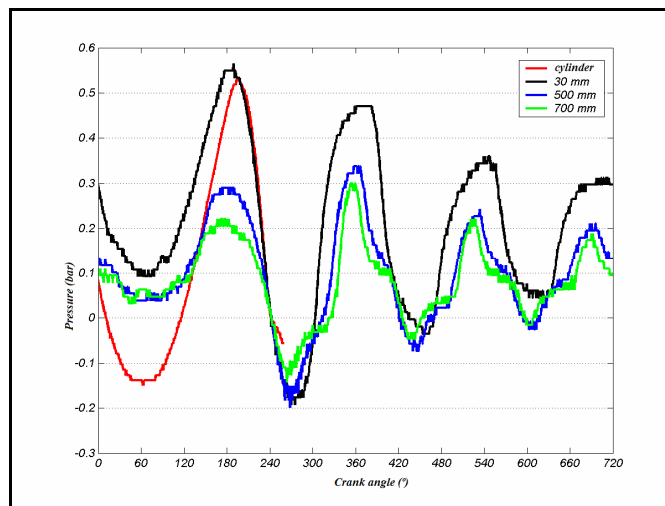Figure 10 – Pressure variation in the admission duct (2600 rpm).

Figure 11 - Pressure variation in the exhaust duct (2400 rpm).

Figure 11 shows the pressure variation in the exhaust duct for a rotation of 2400 rpm. The zero crank angle in this figure corresponds to the beginning of the exhaust valve opening. It can be noticed that at the beginning of the exhaust valve opening the in-cylinder pressure is low, causing the entrance of mass into the cylinder through the exhaust valve. This behavior is opposite to the normal engine operation and would not occur if the experiment had been done with the engine running fired. After passing the bottom dead center, the piston goes up and the pressure in the cylinder increases forming a compression wave. It is interesting to note that the format of the wave propagated along the exhaust duct is unchanged after the closing of the valves, only varying in amplitude. This is due to the fact that there is no further pressure excitement in the cylinder and the pressure at the other end of the duct is almost constant (atmospheric pressure).

Figures 12 and 13 show the influence of the engine speed on the pressure waves in the admission and exhaust ducts, respectively. The chosen position was the one nearest to the valve (30 mm), for it presents the greatest amplitude. As expected, both the amplitude and the frequency vary with the rotation speed of the driving-shaft. As the rotation increases so does the in-cylinder pressure and, therefore, the amplitude of the pressure wave that is propagated along the duct also increases.
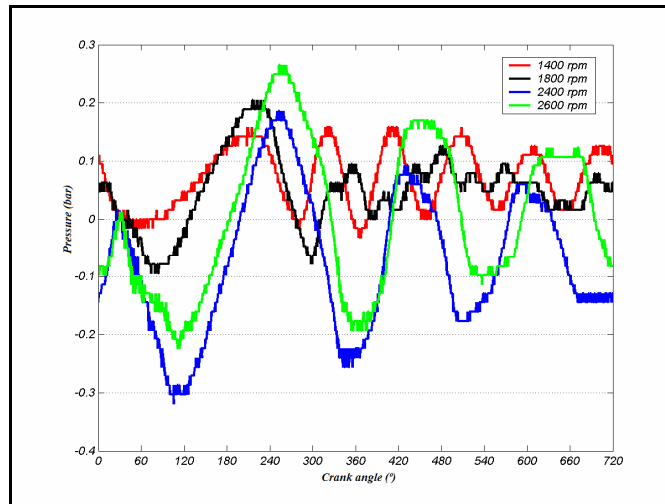
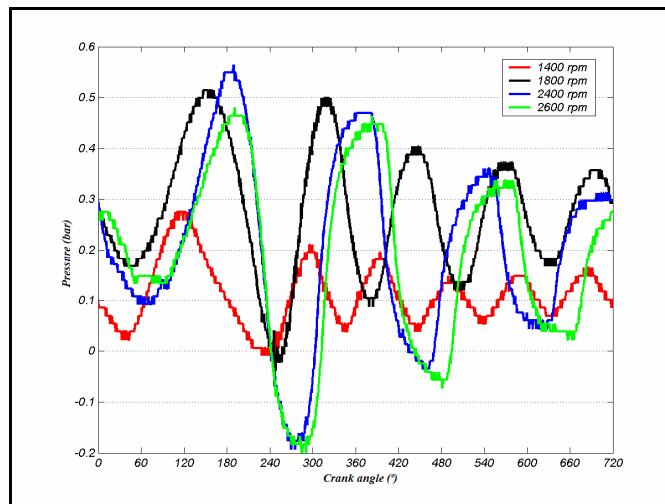Figure 12 – Pressure oscillations at admission duct position of 30 mm.

Figure 13 – Pressure oscillations at exhaust duct position of 30 mm

4. CONCLUSIONS

This project presented the construction of a test bench that allows for the study of the pressure waves that propagate in the admission and exhaust ducts of a single-cylinder motored engine. It also contains the description of the measuring instruments that were used, their working principles and the necessary precautions that need to be taken into consideration during the experiments.

With respect to the system of measuring the valve displacement, it is worth mentioning the ease of its application when the admission and exhaust valves can be accessed without difficulty, as in the case of the engine that was used. Automobile engines that have valves in the cylinder head should also permit easy access to the valves.

The piezoelectric transducers proved to be adequate for the pressure measurements of the present study, the only problem being the lack of a pressure reference. This characteristic is inherent to piezoelectric pressure sensors, due to the fact that they only measure pressure variations. Despite this lack of reference, the information collected in this experiment satisfy the main goal of the work, which is the obtainment of experimental data for future comparison with the results supplied by a computational model.

The obtained pressure data adequately represent the physics of the wave propagation in ducts. However, a considerable improvement in the quality of these experimental data could be obtained by using a piezoelectric transducer of higher sensitivity.

A numerical model validated using the data supplied by the described physical model would permit to analyze the influence of geometric parameters of the admission and exhaust ducts (transversal section area, the variation of this area along the duct, length of the ducts, etc.) on parameters such as the volumetric efficiency and the residual gas fraction.

Such a model will also allow for an optimization of the valves timing as well as the geometry of the admission and exhaust ducts.

5. REFERENCES

AVL List GmbH, AVL 617 Indimeter: operation instructions, Graz-Austria, 1994.

Bueno, A. V. Análise da operação de motores diesel com misturas parciais de biodiesel, PhD thesis, Mechanical Engineering Faculty of the State University of Campinas, 2006.

Heywood, J. B., Internal combustion engine fundamentals, McGraw-Hill, New York, 1988.

Lancaster, D.R., Krieger, R.B. and Lienesch, J.H., Measurement and analysis of engine pressure data, SAE Paper 750026, 1975.

Lapuerta, M., Armas, O., and Bermúdez, V. Sensitivity of diesel engine thermodynamic cycle calculation to measurement errors and estimated parameters, Applied Thermal Engineering 20 (2000) 843-861.

Payri, F., Molina, S., Martín, J. and Armas, O. Influence of measurement errors and estimated parameters on combustion diagnosis, Applied Thermal Engineering 26 (2006) 226-236.

Velásquez, J. A. Simulação dos processos e análise exergética dos motores de ciclo diesel, PhD thesis, Mechanical Engineering Faculty of the State University of Campinas, 1993.